Journal of proteome research

pubs.acs.org/jpr

Article

ARID3C Acts as a Regulator of Monocyte-to-Macrophage Differentiation Interacting with NPM1

Hui-Su Kim, Yong-In Kim, and Je-Yoel Cho*

Cite This: *J. Proteome Res.* 2024, 23, 2882−2892

Read Online

ACCESS | Metrics & More | Article Recommendations | Supporting Information

ABSTRACT: ARID3C is a protein located on human chromosome 9 and expressed at low levels in various organs, yet its biological function has not been elucidated. In this study, we investigated both the cellular localization and function of ARID3C. Employing a combination of LC-MS/MS and deep learning techniques, we identified NPM1 as a binding partner for ARID3C's nuclear shuttling. ARID3C was found to predominantly localize with the nucleus, where it functioned as a transcription factor for genes STAT3, STAT1, and JUNB, thereby facilitating monocyte-to-macrophage differentiation. The precise binding sites between ARID3C and NPM1 were predicted by AlphaFold2. Mutating this binding site prevented ARID3C from interacting with NPM1, resulting in its retention in the cytoplasm instead of translocation to the nucleus. Consequently, ARID3C lost its ability to bind to the promoters of target genes, leading to a loss of monocyte-to-macrophage differentiation. Collectively, our findings indicate that ARID3C forms a complex with NPM1 to translocate to the nucleus, acting as a transcription factor that promotes the expression of the genes involved in monocyte-to-macrophage differentiation.

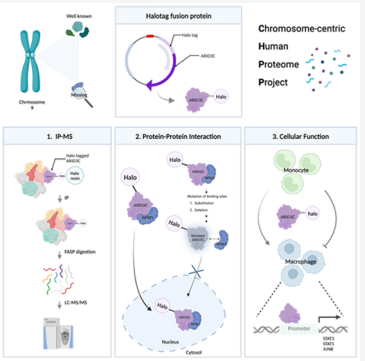

KEYWORDS: *ARID3C, NPM1, LC-MS/MS, AlphaFold2, interactome analysis, monocyte differentiation, Chromosome-centric Human Proteome Project*

INTRODUCTION

Protein analysis plays a pivotal role in understanding cellular processes, disease mechanisms, and biomarker discovery. However, according to the latest version of neXtProt DB, (released on April 18, 2023) as a result of numerous studies, it has been revealed that 18,397 out of 20,389 coding genes in humans, which constitutes 90% of the total, have evidence at the protein level. This discovery began with the Chromosome-centric Human Proteome Project (C-HPP), initiated by the Human Proteome Organization (HUPO) in 2012, to identify missing proteins (MPs) and characterize the protein's role encoded by each chromosome. Proteins are categorized into five levels according to their protein existence (PE), ranging from experimental evidence at the protein level (PE1) to experimental evidence at the transcript level (PE2), protein inferred from homology (PE3), protein predicted (PE4), and protein uncertain (PE5). The number of MPs and uncharacterized PEs still existed, and they are considered to be in the "dark field" of proteomics research. Over the years, significant advancements in coupled high-performance liquid chromatography (HPLC)- and mass spectrometry (MS)-based techniques have revolutionized the field of protein analysis, enabling more comprehensive and in-depth investigations.[1] MS-based approaches also provide a quantitative analysis, along with the capability to detect post-translational modifications[2] and analyze complex mixtures.[3] These technological advancements have facilitated research on proteins that were previously challenging to study using traditional methods.[4] Consequently, the number of proteins with confirmed existence has increased from 15,649 to 18,397 over the past decade (as of April 18th, 2023 released in neXtProt). Alongside the advancements in MS technology, there is a growing interest in employing deep learning approaches for protein analysis.[5] Integration of these two approaches has enhanced our ability to study protein structure, function, and interactions. In this study, we employed MS and deep learning-based AlphaFold2[6,7] to investigate the interactome and its function of the partially studied protein ARID3C (AT-rich interactive domain-containing protein 3C).

ARID3C is located in the human chr 9p13.3 and categorized as the PE1 level, but its molecular function in cells has not been fully elucidated yet except in B cells.[8] ARID3C is a member of the AT-rich interaction domain 3 (ARID3) transcription family consisting of two functional domains that play a major role in its function. The first one is the ARID domain, which is known to bind to DNA,[9] and the other is the REKLES domain, which is known to be involved in nuclear

Special Issue: Women in Proteomics and Metabolomics

Received: August 12, 2023
Revised: December 15, 2023
Accepted: December 21, 2023
Published: January 17, 2024

import/export.[10] Other ARID3 family ARID3A localized on chromosome 19 and was reported to have various functions in embryonic development,[11] immune,[12] and cancers.[13−15] Unlike ARID3A, only one study reported that ARID3C was shown to participate in the immunoglobin gene transcription in B cells.[8] Tidwell et al. revealed that the mouse homologue of human ARID3C, referred to as Brightlike, is expressed in B lineage lymphocytes, undergoes nuclear-cytoplasmic shuttling, associates with Bright (ARID3A), and acts as a coactivator for Bright (ARID3A) dependent IgH transcription. However, the function of ARID3C in monocyte-to-macrophage differentiation is unknown. In this study, we employed a combination of LC-MS/MS and a deep learning model to unravel the interacting partners, cellular localization, and molecular functions of ARID3C during the process of monocyte-to-macrophage differentiation.

EXPERIMENTAL SECTION

Cell Culture and Differentiation

Human embryonic kidney (HEK) 293T cell lines and leukemia cell lines THP-1 and HL-60 were obtained from the Korean Cell Line Bank (KCLB; Seoul, Korea). HEK293T cells were maintained in Dulbecco's modified Eagle medium (DMEM, HyClone Laboratories Inc., Logan, Utah, USA), and both leukemia cell lines were maintained in RPMI-1640 (HyClone Laboratories Inc., Logan, Utah, USA) containing 10% fetal bovine serum (HyClone, Waltham, MA, USA) and a 1% antibiotic/antimycotic solution (Gibco, Life Technologies Corp., NY, USA) at 37 °C in a 5% CO_2 condition. The monocyte-to-macrophage differentiation of THP-1 and HL-60 was induced with phorbol 12-myristate 13-acetate (PMA). PMA was added to a final concentration of 0.1 μM for 1×10^6 cells of THP-1 and 2×10^6 cells of HL-60.

RNA Isolation, cDNA Synthesis, and Real-Time PCR Assay

The real-time PCR assay was performed as previously described.[16] Briefly, quantitative RT-PCR was performed in a CFX Connect Real-Time PCR System (Biorad, CA, USA) using Go Taq polymerase (Promega, WI, USA). The PCR conditions were 5 min at 95 °C, followed by 35 cycles of 95 °C for 30 s, 61 °C for 30 s, and 72 °C for 30 s. The comparative Ct method was used for analyzing data with GAPDH serving as an internal normalization control. For real-time PCR analysis, we designed the primer to amplify the exon−exon junction of a gene of interest. The specific primer sets are provided in Table S1.

Western Blotting Assay

The Western blotting assay was performed as previously described.[17] Information on antibodies used in the study is provided in Table S1.

Mutagenesis

To construct ARID3C proteins with a deletion in the REKELES β domain and four amino acid substitutions, site-directed mutagenesis was performed with a Q5 Site-Directed Mutagenesis Kit following the manufacturer's instructions (New England Biolabs, Ipswich, MA, USA). Primers used for Q5 site-directed mutagenesis were designed using the NEBase Changer tool (https://nebasechanger.neb.com/). In brief, deletion and substitution primers were employed for exponential amplification followed by the use of the kinase-ligase-Dpn1 (KLD) enzyme to remove the template. Subsequently, plasmids were obtained through transformation using competent *E. coli*.

The substituted amino acids were chosen based on the principles of "Grantham's distance", "Sneath's distance", and "Miyata's distance", selecting the amino acid with the greatest difference, dissimilarity, and distance, producing the V381D, F383D, A384W, and R385G mutants.

HaloTag Protein Purification

HEK293T cells were transfected with 10 μg of N-term Halo tagged ARID3C plasmid DNA using a NEPA21 electroporator (Nepagene, Chiba, Japan) with following the manufacturer's instructions (Voltage; 150 V, Pulse; 5 ms). The detailed structure of the HaloTag ARID3C plasmid is provided in Figure S1, ordered from Promega (ORF clone #FHC02454). Two days after transfection, HEK293T cells were harvested with a mammalian lysis buffer (50 mM Tris−HCl, pH 7.5, 150 mM NaCl, 1% Triton X-100, and 0.1% sodium deoxycholate) supplemented with a protease inhibitor cocktail. Lysate was cleared by centrifugation, and the supernatant was incubated with the pre-equilibrated resin for 15 min at room temperature (RT) with rotation. After incubation, the resin was washed four times with a mammalian lysis buffer. Then, two different methods of elution were used for immune blot and interactome analysis. For the immunoblotting, the resin was resuspended with a SDS elution buffer (50 mM Tris−HCl, pH 7.5, and 1% SDS) and boiled for 10 min at 100 °C. For interactome analysis, the resin was resuspended with TEV protease for 20 min with rotation in RT to cleave ARID3C with HaloTag, and TEV protease was removed by incubation with MagneHis Ni-Particles. Tag-free proteins were analyzed by LC-MS/MS.

Filter-Aided Sample Preparation (FASP) and Mass Spectrometry (MS) Analysis

Interactome proteins eluted from HaloTag purification were digested with trypsin following the FASP protocol.[18] The peptide was cleaned up and fractionated using poly(styrene-divinylbenzene)-reversed-phase sulfonate (SDB-RPS) Stage-Tips performed as previously described.[19] Briefly, LC-MS/MS analysis was performed with an Orbitrap Fusion Lumos mass spectrometer (Thermo Fisher Scientific, IL, USA) coupled with an EASY-nLC1200 UHPLC (Thermo Fisher Scientific). The sample was injected into an EASY-Spray column (75 μm i.d. × 50 cm; PepMap RSLC C18 particle, 2 μm particle size, 100 Å pore size, Thermo Fisher Scientific) followed by a 120 min LC gradient at a flow rate 300 nL min^{-1}. MS measurements were acquired by data-dependent mode with a 3 s cycle time during the HPLC separation. Raw data were processed with MaxQuant (v. 1.6.5.1) software, and a threshold was set to a 1% false discovery rate (FDR) for both PSM and protein. The UniProt human proteome (number of entries: 20,423) was used for database searching. In this study, the criteria that followed the HUPO guidelines were used for data analysis and protein identification. The proteins were identified with two or more unique peptides (>9 amino acids). Raw data was deposited at https://massive.ucsd.edu/ProteoSAFe/static/massive.jsp?task=7c82d864a7a24a7eb8afc824744a7e88 (MassIVE MSV000093593).

Chromatin Immunoprecipitation (ChIP)

The Halo ChIP system was performed with the HaloCHIP system following the manufacturer's instructions (Promega,

https://doi.org/10.1021/acs.jproteome.3c00509
J. Proteome Res. 2024, 23, 2882−2892

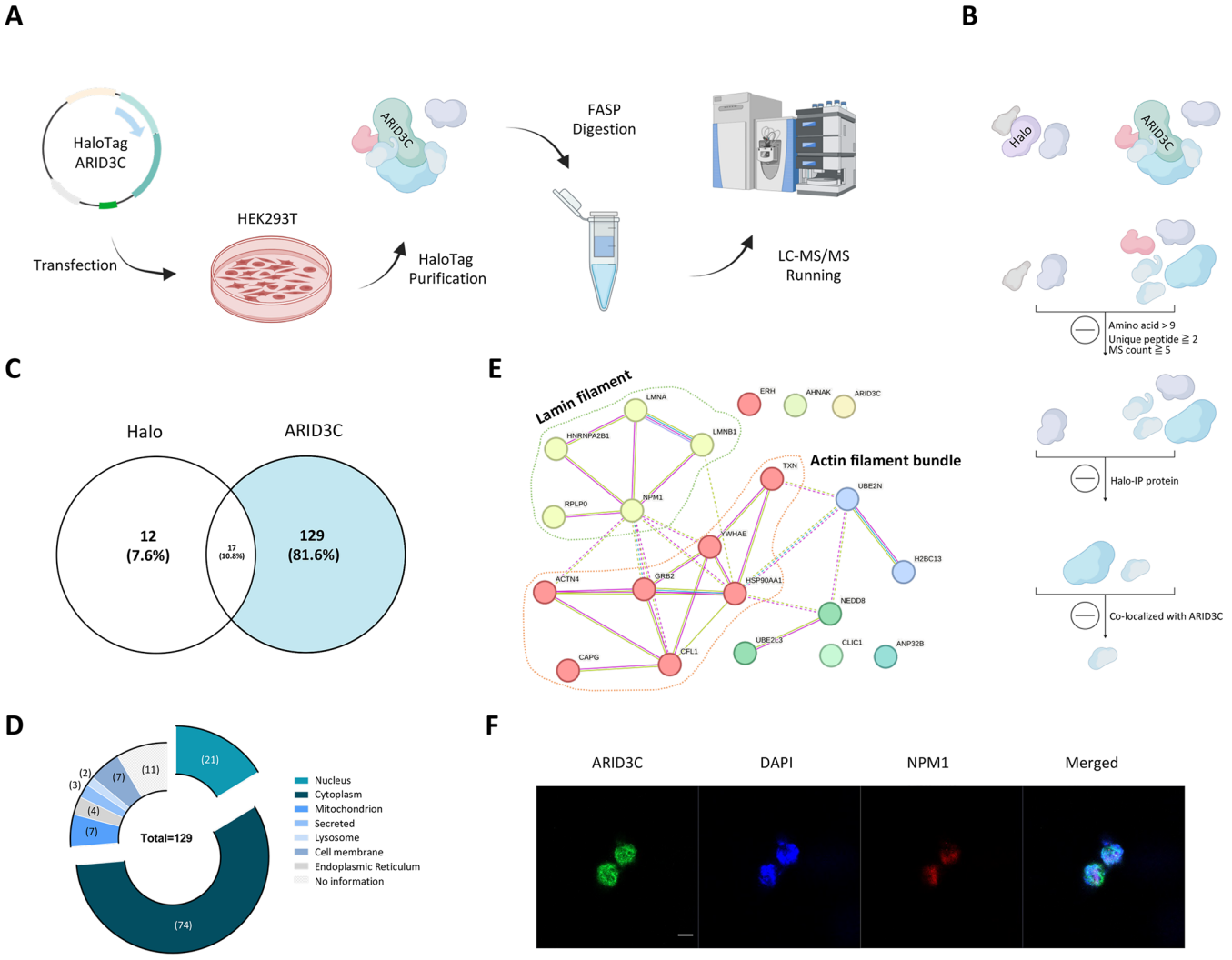

Figure 1. Interactome analysis of ARID3C. (A) Strategy to identify interaction partners of ARID3C. HEK293T cells used for ARID3C overexpression and the purified ARID3C complex by HaloTag purification were digested into peptides using the FASP digestion method for LC-MS/MS. (B) Schematic illustration of the ARIC3C interactome analysis. To identify the ARID3C binding partner, we filtered out proteins that were expected to be false positive under 3 step conditions. (C) Venn diagram showing the distribution of the total 158 candidates selected. (D) Distribution of the subcellular localization of selected 129 candidates. (E) Protein−protein interaction (PPI) network of the proteins specific to ARID3C interactome and predicted to be present with the nucleus. (F) Representative images showing the subcellular localization of ARID3C and NPM1. Double immunofluorescence staining shows colocalization between ARID3C and NPM1 in the nucleus. Scale bar: 10 μm. Figure 1A,B created with BioRender.com.

WI, USA, #G9410). Briefly, transfected 293T cells were cross-linked with formaldehyde (final concentration; 1%) and DNA was sonicated to a size of 500−2,000 bp using a Bioruptor Pico sonicator (Diagenode, Paris, France) for 10 cycles of 30 s on; 30 s off, followed by centrifugation at a high speed for 5 min. Supernatants were incubated with pre-equilibrated resin for 2 h with mixing at RT. The resin was washed subsequently with a mammalian lysis buffer, nuclease-free water, a high salt wash buffer, and nuclease-free water. Captured DNA was reverse cross-linked by adding a reversal buffer for 12 h at 65 °C and eluted DNA was cleaned up with a Fragment DNA purification Kit (iNtRON Biotechnology, Seongnam, Korea). The purity and quantity of isolated DNA were measured by the ratio of 260/280 nm absorbance, and 1 ng of DNA was used for PCR.

Flow Cytometry

PMA-treated HL-60 and THP-1 cells were detached and rinsed with PBS two times. The cell pellets were resuspended with a cell staining buffer (BioLegend) and incubated with the primary antibody; CD11b for 15 min at 4 °C. After the cells were washed with a cell staining buffer, the cells were incubated with the secondary antibody at 4 °C for 15 min. To remove dead cells, 7-AAD was added, and the samples were analyzed with FACS AriaII (BD Biosciences, NJ, USA). Information on antibodies used in study is provided in Table S1.

Immunostaining

Immunostaining was done as described previously.[16] Briefly, HEK293T cells were fixed with 4% paraformaldehyde and permeabilized with 0.5% Triton X-100 in PBS. After a washing treatment with PBS/T, the cells were blocked with 5% BSA and incubated primary antibodies for 1 h at room temperature. Secondary antibodies were incubated for 1 h at room temperature, and nuclei counterstaining was performed using 1 μg/mL DAPI (Thermo Fisher Scientific, MA, USA). Information on the used antibodies is provided in Table S1.

https://doi.org/10.1021/acs.jproteome.3c00509
J. Proteome Res. 2024, 23, 2882−2892

Table 1. List of 129 Proteins Identified Only in ARID3C

	Log2 (LFQ intensity)						
	ARID3C_1	ARID3C_2	Halo_1	Halo_2	Number of unique peptides	Number of MS/MS count	Majority protein IDs (Uniprot)
1	30.12	30.0044	NaN	NaN	19	179	P08670
2	28.4604	28.2145	NaN	NaN	13	133	P62258
3	30.2252	30.1298	NaN	NaN	17	128	P13796
4	30.5858	30.6375	NaN	NaN	10	128	P62937
5	29.9687	29.8311	NaN	NaN	7	112	P62328
6	28.3572	28.233	NaN	NaN	13	110	P12814
7	29.404	29.3822	NaN	NaN	10	100	P63104
8	32.0579	32.0949	NaN	NaN	20	96	A6NKF2
9	30.2802	30.2902	NaN	NaN	4	84	P15090
10	29.9453	29.7907	NaN	NaN	11	81	P0DP25
11	28.906	28.8909	NaN	NaN	7	78	P08238
12	27.1048	27.0888	NaN	NaN	18	58	P35579
13	27.9159	28.046	NaN	NaN	9	57	P29401
14	27.206	27.1318	NaN	NaN	16	56	P55072
15	27.1571	26.9163	NaN	NaN	15	53	P53396
16	27.2145	27.115	NaN	NaN	15	52	P11021
17	27.2572	27.2982	NaN	NaN	11	51	Q9BQE3
18	27.2042	27.0744	NaN	NaN	9	50	P06733
19	27.4809	27.3402	NaN	NaN	11	49	P22626
20	26.7021	26.792	NaN	NaN	8	48	P04075
21	27.2727	27.5049	NaN	NaN	13	48	P14618
22	28.506	28.59	NaN	NaN	3	47	P22392
23	27.2013	27.202	NaN	NaN	8	44	O75083
24	26.4315	26.3275	NaN	NaN	21	44	P21333
25	28.5898	28.4875	NaN	NaN	7	43	Q99880
26	29.063	29.0558	NaN	NaN	7	42	P40925
27	26.7091	26.7141	NaN	NaN	7	39	P40926
28	26.7967	26.5888	NaN	NaN	6	37	P37802
29	26.4339	26.5495	NaN	NaN	15	37	P38646
30	27.0824	27.0201	NaN	NaN	9	36	P18669
31	27.6382	27.8432	NaN	NaN	8	36	P23528
32	28.0646	28.0349	NaN	NaN	4	36	Q14019
33	26.8818	27.0149	NaN	NaN	6	35	P52565
34	28.6161	28.5627	NaN	NaN	5	34	P07451
35	29.2086	29.0912	NaN	NaN	4	34	P62987
36	26.1365	26.1635	NaN	NaN	8	34	P27797
37	26.9203	26.8601	NaN	NaN	6	34	P50395
38	28.4068	28.3238	NaN	NaN	3	33	Q9H299
39	26.2729	26.3007	NaN	NaN	6	32	P49327
40	25.7337	25.7989	NaN	NaN	7	31	P26641
41	27.0896	27.0654	NaN	NaN	6	31	P61981
42	26.743	26.6946	NaN	NaN	5	31	Q01105
43	26.0515	26.1457	NaN	NaN	7	30	P26038
44	25.9424	25.9155	NaN	NaN	9	29	P02545
45	26.4487	26.4448	NaN	NaN	5	29	P48163
46	24.5694	23.1841	NaN	NaN	2	28	P31946
47	25.923	25.8683	NaN	NaN	12	27	O43707
48	27.3689	27.5557	NaN	NaN	6	27	P67936
49	26.6154	26.3999	NaN	NaN	4	26	O14818
50	25.6329	25.6336	NaN	NaN	6	26	P00558
51	24.8373	26.393	NaN	NaN	2	26	P07737
52	26.0769	25.7863	NaN	NaN	5	26	P09960
53	28.5898	28.5863	NaN	NaN	2	26	P69905
54	26.2238	26.0614	NaN	NaN	3	25	O75368
55	25.453	25.5016	NaN	NaN	10	24	P13639
56	26.0734	26.1436	NaN	NaN	5	24	P14550
57	26.0511	25.9075	NaN	NaN	7	24	P60900
58	22.714	22.2538	NaN	NaN	3	24	Q14847
59	25.4443	25.5144	NaN	NaN	6	24	Q16555

https://doi.org/10.1021/acs.jproteome.3c00509
J. Proteome Res. 2024, 23, 2882−2892

Table 1. continued

	Log2 (LFQ intensity)						
	ARID3C_1	ARID3C_2	Halo_1	Halo_2	Number of unique peptides	Number of MS/MS count	Majority protein IDs (Uniprot)
60	25.9694	26.0793	NaN	NaN	6	23	P60660
61	26.4421	26.4004	NaN	NaN	5	22	P06753
62	26.1642	25.9491	NaN	NaN	5	22	P28066
63	25.732	26.1175	NaN	NaN	6	22	P62906
64	23.1074	22.2677	NaN	NaN	5	21	P00450
65	25.8799	25.8317	NaN	NaN	6	21	P25789
66	25.1953	24.8988	NaN	NaN	6	21	P47756
67	26.8839	26.9795	NaN	NaN	5	19	P17066
68	25.6537	25.7283	NaN	NaN	5	19	P25788
69	25.9986	26.0869	NaN	NaN	6	19	Q09666
70	25.1512	24.9405	NaN	NaN	3	19	Q96CX2
71	25.7885	25.9526	NaN	NaN	4	18	P20700
72	26.0504	26.279	NaN	NaN	6	18	P21796
73	24.0385	24.1862	NaN	NaN	9	18	Q13813
74	23.6282	24.3248	NaN	NaN	4	17	P10599
75	25.4717	25.2458	NaN	NaN	4	17	P20618
76	25.5331	25.5971	NaN	NaN	4	17	P30041
77	24.9751	24.827	NaN	NaN	5	16	P05387
78	25.6952	25.6926	NaN	NaN	5	16	P27348
79	25.1294	25.1703	NaN	NaN	5	16	P30050
80	24.5228	24.6406	NaN	NaN	3	15	P07237
81	25.5825	25.4838	NaN	NaN	6	15	P07900
82	24.9059	24.9505	NaN	NaN	4	15	P31146
83	24.7428	24.6945	NaN	NaN	4	15	P61978
84	25.4134	25.4558	NaN	NaN	5	15	Q04917
85	25.2021	25.3364	NaN	NaN	3	14	P06748
86	26.5516	26.5969	NaN	NaN	2	14	P09382
87	24.4993	24.392	NaN	NaN	4	14	P17661
88	24.9741	24.9066	NaN	NaN	5	14	P68036
89	25.6818	25.5923	NaN	NaN	4	14	Q01518
90	24.1792	24.2282	NaN	NaN	4	13	O00299
91	24.1186	23.6956	NaN	NaN	2	13	P07437
92	25.2535	25.1577	NaN	NaN	5	13	P25786
93	26.2894	24.4252	NaN	NaN	3	13	P31150
94	25.6275	25.6403	NaN	NaN	3	13	P84090
95	25.1939	25.0022	NaN	NaN	2	12	P49720
96	26.3338	26.1736	NaN	NaN	2	12	P62942
97	24.5106	24.4904	NaN	NaN	3	12	P62993
98	24.5391	24.3048	NaN	NaN	7	12	Q00610
99	25.1356	25.441	NaN	NaN	3	12	Q01469
100	24.409	24.623	NaN	NaN	2	12	Q92688
101	23.5913	23.7504	NaN	NaN	4	11	P00492
102	24.7287	24.5849	NaN	NaN	5	11	P25705
103	25.3262	25.4438	NaN	NaN	3	11	P30086
104	25.7681	25.8786	NaN	NaN	2	11	P63313
105	24.5665	24.8052	NaN	NaN	3	10	Q96KP4
106	24.0623	23.8665	NaN	NaN	5	9	P00390
107	23.201	23.1414	NaN	NaN	2	9	P30044
108	23.7605	23.5635	NaN	NaN	2	9	P40121
109	25.5797	25.7457	NaN	NaN	5	9	P45880
110	24.6042	24.509	NaN	NaN	4	9	P59998
111	24.8658	24.5847	NaN	NaN	2	9	Q99497
112	24.1469	24.2116	NaN	NaN	2	8	P00167
113	23.0005	22.9948	NaN	NaN	4	8	P07195
114	23.2701	22.9133	NaN	NaN	2	8	P07339
115	27.1996	27.0812	NaN	NaN	2	8	P07602
116	24.4011	24.3697	NaN	NaN	2	8	P29218
117	23.4316	23.0263	NaN	NaN	4	8	P46940
118	23.6986	23.7716	NaN	NaN	4	8	P63010

https://doi.org/10.1021/acs.jproteome.3c00509
J. Proteome Res. 2024, 23, 2882−2892

Table 1. continued

	Log2 (LFQ intensity)						
	ARID3C_1	ARID3C_2	Halo_1	Halo_2	Number of unique peptides	Number of MS/MS count	Majority protein IDs (Uniprot)
119	24.5091	25.1422	NaN	NaN	3	8	Q08554
120	23.1579	23.2595	NaN	NaN	5	7	P05388
121	23.2641	23.1863	NaN	NaN	2	7	P61088
122	23.0243	22.6641	NaN	NaN	2	6	P02790
123	23.8524	23.8998	NaN	NaN	3	6	P23526
124	22.6404	22.507	NaN	NaN	2	6	P61158
125	23.684	24.0302	NaN	NaN	2	6	Q15843
126	23.1316	23.1095	NaN	NaN	3	5	O15144
127	22.9613	22.9744	NaN	NaN	3	5	P06737
128	22.8313	22.6406	NaN	NaN	3	5	P15121
129	23.511	23.6221	NaN	NaN	2	5	Q9NZT1

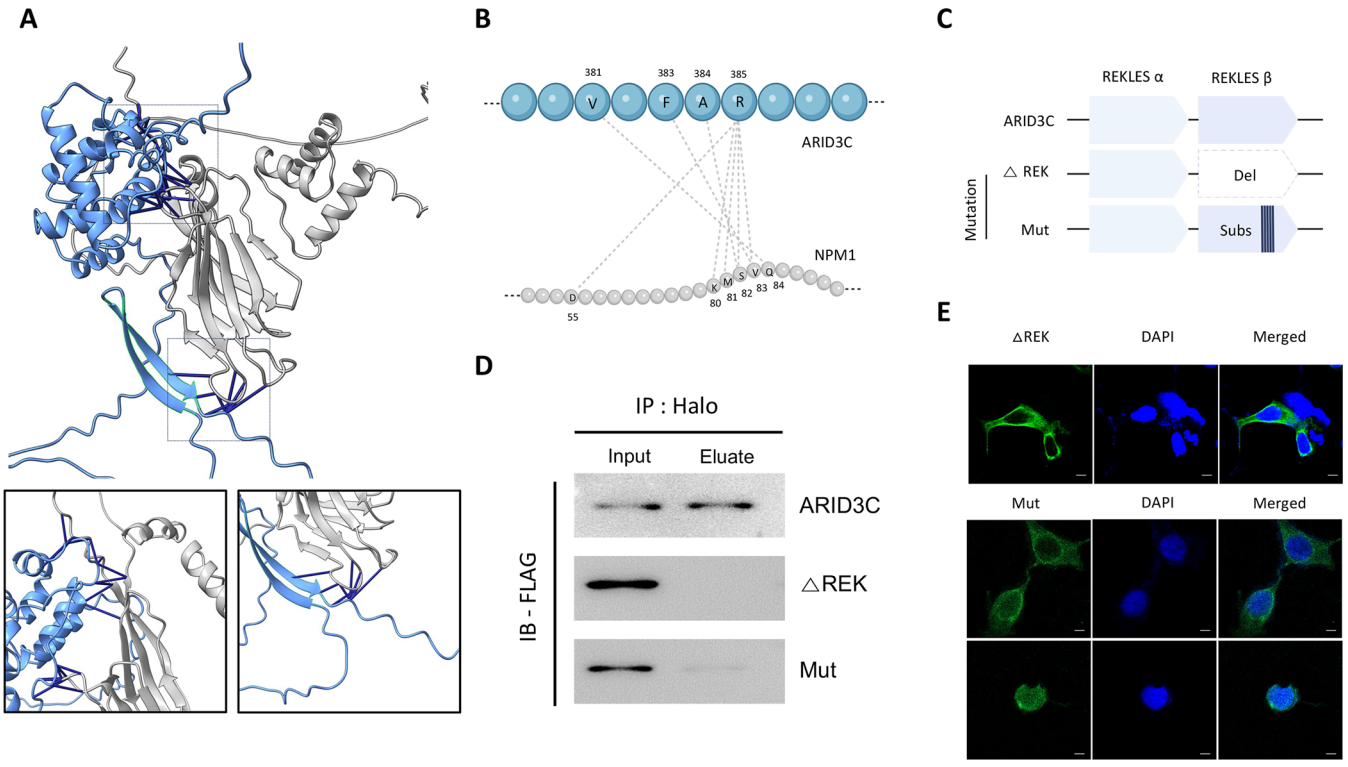

Figure 2. ARID3C interacts with NPM1 for nuclear shuttling. (A) Predicted 3D structure of ARID3C and NPM1 interaction complex revealed by AlphaFold2. Blue, ARID3c; Gray, NPM1. Residue−residue alignment confidence (PAE) contacts were labeled with dark blue. Magnified left image, binding site between ARID domain of ARID3C and NPM1; right image, REKLES β domain of ARID3C and NPM1. (B) Structure of REKLES β domain amino acids of ARID3C and the corresponding amino acids of NPM1. (C) Structure of the deletion and amino acid substitution mutated in REKES β domain. (D) Coimmunoprecipitation assay with ARID3C, ΔREK, and Mut with Halo antibody verified the interaction between ARID3C and NPM1. (E) Representative images showing the subcellular localization of mutated ARID3C and NPM1. Scale bar: 10 μm. Figure 2B created with BioRender.com.

Bioinformatic Analysis

Protein−protein interaction (PPI) network analysis was conducted with the STRING DB (v. 11) (https://string-db.org/). The proteins were classified using the UniProt database based on their subcellular location. AlphaFold2 v. 2.2.0 generates a PDB file based on the full sequence of the protein.[7] The best model from the generated PDB file was utilized for standard molecular visualization. Structure figures were visualized using UCSF ChimeraX v.1.2.5 developed by the Resource for Biocomputing, Visualization, and Informatics at the University of California, San Francisco, with support from National Institutes of Health R01-GM129325 and the Office of Cyber Infrastructure and Computational Biology, National Institute of Allergy and Infectious Diseases.[20] The average shortest distance between protein and protein is 4.0 Å.

Statistical Analysis

Statistical analysis was performed using Prism software (v. 8.0.1, GraphPad Software). For the statistical significance of multiple groups, 2-way ANOVA combined with Tukey's honest significant difference (HSD) test was performed, and Student's t test was performed for analysis between two groups. The data represent means ± SEM. Significant differences are indicated with different letters in each figure legend.

https://doi.org/10.1021/acs.jproteome.3c00509
J. Proteome Res. 2024, 23, 2882−2892

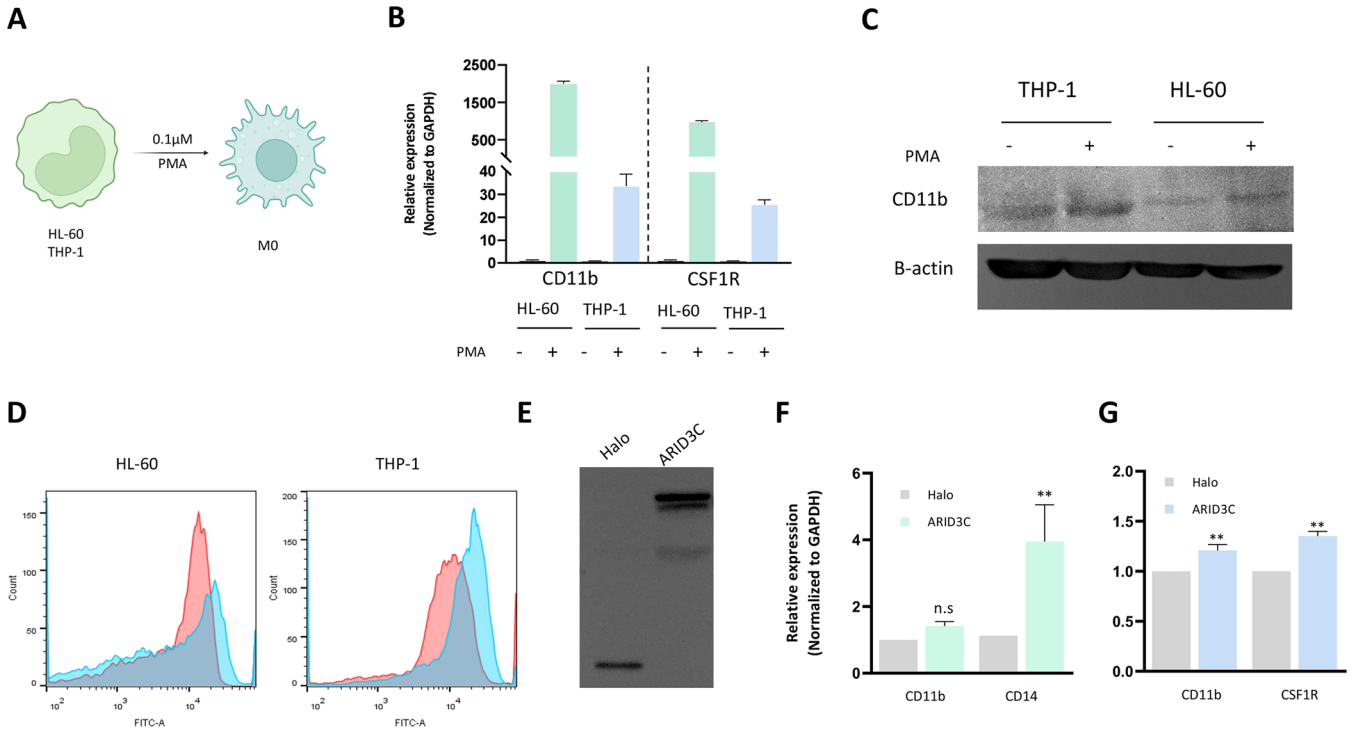

Figure 3. ARID3C induce monocyte-to-macrophage differentiation. (A) Graphical representation of monocyte differentiation into macrophages induced by phorbol-12-myristate-13-acetate (PMA). (B) Relative mRNA expression of CD11b and CSF1R for monocyte-to-macrophage differentiation was quantified by qRT-PCR. The results were analyzed using 2−ΔΔCT and GAPDH as a reference gene. (C) Protein expression level of CD11b quantified by Western Blot. β-Actin was used as an internal control. (D) Representative flow cytometry of CD11b of monocyte and PMA treated monocytes. (E) Halo and ARID3C overexpressed cells were used for Western Blotting. (F,G) Relative mRNA expression of CD11b, CD14, and CSF1R was quantified by qRT-PCR. HL-60 (F) and THP-1 (G) cells were transfected with ARID3C and treated with PMA for 24 h. The results were analyzed using 2−ΔΔCT and used GAPDH as a reference gene. All data are presented as mean ± SEM (n = 3). The Student's t test was used to analyze the data, and statistical analysis was performed. **P < 0.01; n.s., not significant. Figure 3A created with BioRender.com.

RESULTS

Analysis of ARI D3C Interactors by Coimmunoprecipitation and Mass Spectrometry

To identify the interaction partners of ARID3C, we transiently expressed a Halo-tagged ARID3C protein in 293T cells and subsequently purified the tagged protein along with its interactors (Figure 1A and S1A). As a negative control for protein−protein interactions, we used protein extracts from cells expressing the free HaloTag (Figure 1B). Protein identifications from the mass spectrometry were filtered using the criteria of the HUPO guidelines, then proteins commonly identified in the HaloTag control were removed. Moreover, false-positive proteins with predicted cellular localization differing from ARID3C were also excluded.

The IP-MS analysis identified a total of 158 proteins, with a FDR calculation below 1% at the global protein level. One hundred twenty-nine proteins were unique to ARID3C, not overlapping with the HaloTag control (Figure 1C and Table 1). We detected 20 unique peptides of ARID3C, and the MS spectrum is shown in Figure S2A. We conducted PPI analysis using the STRING database, dividing proteins into two groups: all 129 proteins (Figure S3A) and nuclear-localized proteins (Figure 1E). When analyzing the PPIs of the 129 proteins associated with ARID3C, we identified five main clusters: Type III intermediate filament, Proteasome core complex, Dendritic growth core, Muscle thin filament tropomyosin, and Acetyl-CoA carboxylase complex. Notably, nuclear proteins exhibited more specific clustering, particularly involving the lamin filament and actin filament. We focused on proteins that constitute the lamin filament, aiming to better elucidate the role of ARID3C as a transcription factor. Among these lamin filament proteins (NPM1, RPLP0, LMNA, LMNB1, and HNRNPA2B1), we emphasized NPM1, which occupies the most nodes. Furthermore, ARID3C and NPM1 are colocalized in the nucleus in the 293T cells (Figure 1E). Thus, in this study, we focused on the interaction between ARID3C and NPM1.

ARID3C Interacts with NPM1 for Nuclear Shuttling

Next, we employed AlphaFold2 to predict the 3D structures of the ARID3C and NPM1 protein (Figure S4A,B) and predicted its interaction with NPM1 (Figure 2A). Based on the report that NPM1 is involved in nuclear shuttling,[21] we hypothesized that ARID3C may interact with NPM1 to enter the nucleus. Three-dimensional predictions by AlphaFold2 unveiled that NPM1 interacts with two sites: the ARID domain (left) and the REKLES β domain (right) of ARID3C. As the ARID domain is known to be involved in DNA binding,[9] we focused on the REKLES β domain. Four amino acids, V381, F383, A384, and R385, in the REKLES β domain of ARID3C are predicted to be involved in the binding to NPM1 (Figure 2B). To explore whether ARID3C indeed binds to NPM1, we constructed two different mutations (Figure 2C). The first mutation deleted the whole REKLES β domain including the four amino acids (ΔREK), while the second mutation substituted those four amino acids with different amino acids: V381D, F383D, A384W, and R385G (Mut). We transiently expressed ARID3C, ΔREK, and Mut with the

https://doi.org/10.1021/acs.jproteome.3c00509
J. Proteome Res. 2024, 23, 2882−2892

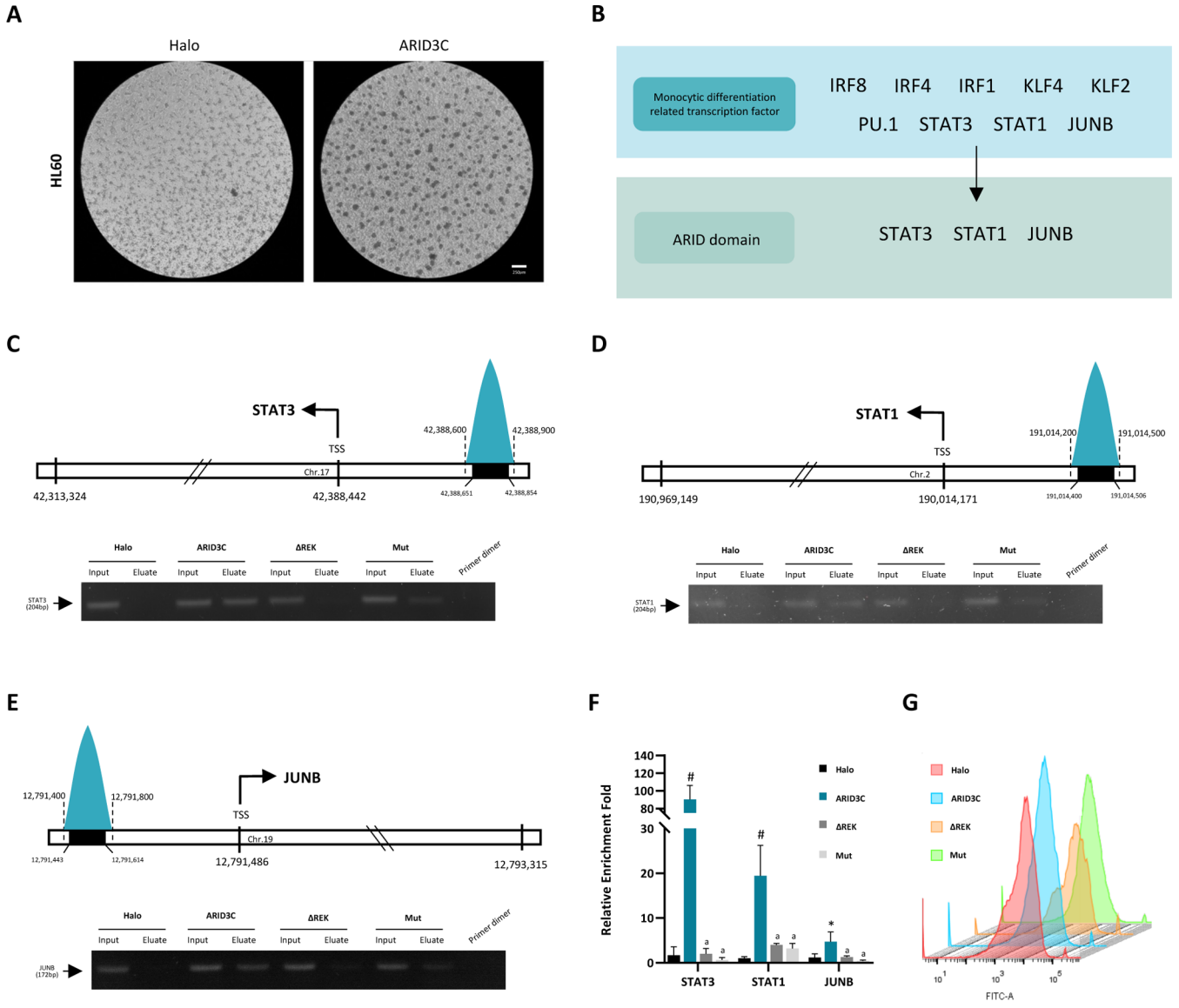

Figure 4. As a transcription factor, ARID3C directly regulates the genes related to macrophage differentiation. (A) Phase contrast microscopy shows that PMA induced HL-60 cells. ARID3C overexpressed HL-60 cell shows morphological characteristics of macrophages. Scale bar: 250 μm. (B) Graphical diagram for selection of transcription factors with an ARID domain related to macrophage differentiation. (C–E) Chromatin immunoprecipitation (ChIP) analysis of STAT3, STAT1, and JUNB in the 293T cells transfected with ARID3C, ΔREK, and Mut. Genome structures of STAT3, STAT1, and JUNB are shown. Blue histogram represents the predicted ARID3C binding domain, and the inner black bar indicates the amplified region by PCR. (F) DNA fold enrichments were quantified by ChIP-qPCR. (G) Expression levels of CD11b in Halo, ARID3C, ΔREK, and Mut transfected HL-60 cells were analyzed by FACS (red, Halo; blue, ARID3C; orange, ΔREK; green, Mut). All data are presented as mean ± SEM (n = 3). The statistical analysis is presented. Two-way ANOVA was used to compare groups. # $p < 0.01$, * $p < 0.05$, and a, not significant.

NPM1-flag in 293T cells. After IP using the HaloTag of ARID3C and performing immunoblotting with the Flag antibody, we found that ARID3C bound to NPM1, while ΔREK did not bind at all. The Mut showed limited binding to NPM1. Herein, we have demonstrated that ARID3C interacts with NPM1 and that the specific four amino acids in the REKLES β domain play a pivotal role in this interaction (Figure 2D).

Next, we investigated the subcellular localization of mutated ARID3C and NPM1. We found that both ARID3C and NPM1 exist in the nucleus of cells, while the deleted ARID3C (ΔREK) is retained in the cytoplasm (Figure 2E). The substitution form of ARID3C (Mut) was found to have both nuclear and cytoplasmic localization, which is reminiscent of the IP-IB result (Figure 2D) with some binding to NPM1 and some not. These observations highlight that the translocation of ARID3C from the cytoplasm to the nucleus is contingent upon its interaction with the REKLES β domain of NPM1, mainly those four amino acids V381, F383, A384, and R385.

ARID3C Promotes PMA-Induced Myeloid Differentiation

To investigate the role of ARID3C in monocyte differentiation, we used AML patient-derived monocyte cell lines HL-60 and THP-1. HL-60 and THP-1 were treated with PMA to induce monocyte-to-macrophage differentiation (Figure 3A). A significant increase was observed in the expression of macrophage differentiation markers, CD11b and CSF1R (Figure 3B). Next, we also confirmed an increase in the level

https://doi.org/10.1021/acs.jproteome.3c00509
J. Proteome Res. 2024, 23, 2882−2892

of protein expression of CD11b upon PMA-induced differentiation in both cell types (Figure 3C). Flow cytometric analysis also showed that the number of CD11b-positive cells increased with PMA treatment (Figure 3D).

Subsequently, we conducted transient transfection of HL-60 and THP-1 with either the ARID3C or Halo control construct. Transfection efficiency was confirmed by a Western blot (Figure 3E). After ARID3C transfection, the cells were treated with PMA for the macrophage differentiation. Intriguingly, the expression of ARID3C led to a further augmentation in the levels of CD11b, CD14, and CSF1R mRNA when compared to the control (Figure 3F,G). These findings collectively indicate that ARID3C experts a positive regulatory effect on the monocyte-to-macrophage differentiation.

As a Transcription Factor, ARID3C Directly Regulates Genes Involved in Monocyte-to-Macrophage Differentiation

After induction for 24 h with PMA, HL-60 cells that were transfected with ARID3C exhibited a higher proportion of mature monocytes (Figure 4A). We investigated whether ARID3C binds to NPM1 and enters to the nucleus to act as a transcription factor. To begin, we conducted a screening for master transcription factor genes that orchestrate the process of monocyte-to-macrophage differentiation.[22] Subsequent to this screening, we identified three genes (STAT3, STAT1, and JUNB) that possess an ARID-binding DNA element within their respective promoters (Figure 4B). Notably, STAT3 is required for monocyte migration and differentiation,[23] while STAT1 promotes macrophage activation and the production of inflammatory cytokines.[24] Moreover, JUNB is known to participate in various cellular processes, including immune regulation and differentiation.[25] Together, these transcription factors contribute to the differentiation of monocytes into functional macrophages. Based on this information, we infer that ARID3C acts as a transcription factor that regulates the expression of three genes, which results in an increase in monocyte-to-macrophage differentiation. Next, we performed chromatin immunoprecipitation by the Halo tag followed by PCR (ChIP-PCR). Additionally, we hypothesized that ARID3C would not function as a transcription factor if it failed to bind with NPM1 and was retained in the cytoplasm. To validate this hypothesis, we transfected both the original ARID3C and a mutated form of ARID3C, and observed their binding to the promoters of STAT3, STAT1, and JUNB (Figure 4C−E). The results showed that ARID3C bound to the promoters. We observed that ARID3C binds to the promoters of STAT3, STAT1, and JUNB, but the ΔREK failed to bind and Mut bound at a very limited level, indicating that ARID3C requires an intact NPM1-binding site to act as a transcription factor in differentiation (Figure 4C−E). In Figure 4F, we also detected failure of binding capacity in mutated ARID3C by ChIP-qPCR. Furthermore, we confirmed failure of intact between ARID3C and NPM1 leads to decrease of differentiation by using flow cytometry to measure the level of CD11b marker in cells transfected with the different ARID3C constructs (Figure 4G). Upon transfection of ARID3C in HL-60 cells, the highest expression of CD11b was observed, whereas the deletion of the REKLES domain in ΔREK resulted in the lowest CD11b expression.

These findings indicate that ARID3C promotes macrophage differentiation by binding to NPM1 and translocating into the nucleus to act as a transcription factor. Overall, we showed that ARID3C promotes monocyte differentiation, but mutated ARID3C reduced differentiation ability. Accordingly, ARID3C induces monocyte-to-macrophage differentiation as a transcription factor by regulating the expression of STAT3, STAT1, and JUNB.

DISCUSSION

The number of PE1 proteins has increased from 15,649 to 18,397 in the past ten years, a remarkable achievement of the Chromosome-based Human Proteome Project (C-HPP) project.[26,27] However, 1,521 (as of April 18th, 2023 released in neXtProt) PE1 proteins still lack functional annotation, and they are considered to be in the "dark field" of proteomics research. Here, we not only provided chromosome 9 located protein evidence but also utilized MS plus deep learning to identify binding motifs of the interactors discovered through IP-MS. Furthermore, we experimentally validated ARID3C-NPM1 interactions and reported on the cellular functions during macrophage differentiation.

Despite lacking NLS and NES peptide sequences, ARID3C can shuttle between the nucleus and cytoplasm by binding to NPM1, which we discovered for the first time. NPM1 is known to be mutated in one-third of adult acute myeloid leukemia (AML) patients.[28] The most common mutation is an insertion of "TCGT", which induces a frameshift in the C-terminal and leads to the addition of one more nuclear export signal (NES). These NPM1 mutation (mtNPM1) results in being localized in the cytosol rather than the nucleus.[29] Cytoplasmic delocalization of mtNPM1 induces the cytoplasmic retention of several nuclear proteins. In AML patient-derived cells, NPM1 forms a complex with master transcription factors of monocyte lineage differentiation, such as PU.1 (also known as SPI1), CEBP1, and RUNX1, to regulate granulocytic differentiation.[30] Therefore, mislocalized mtNPM1 in AML cells prevents monocyte and granulocyte terminal differentiation by cytoplasmic retention of PU.1, leading to the disruption of the formation of the PU.1/RUNX1/CEBPA master transcription factor complex.[30] Additionally, the CCCTC-binding factor (CTCF) has been reported to interact with both NPM1 and mtNPM1, but the interaction with mtNPM1 also results in the mislocalization of CTCF.[31] Moreover, mtNPM1 also contributes to the mislocalization of several nuclear proteins such as MIZ1, Fbwγ, and HEXIM1. Likewise, ARID3C has two regions that can bind to NPM1. Inferring from the high prevalence of NPM1 mutations in AML patients, it is reasonable to anticipate that these mutations may also affect the subcellular mislocalization of ARID3C. Further investigation into the potential effects of NPM1 mutations on ARID3C's subcellular localization and its functional implications in AML pathogenesis would be valuable to understand the complex interplay between these proteins in cancer development.

Furthermore, while our focus was on the interaction partners involved in the nuclear import of ARID3C, IP-MS data suggest the existence of additional potential interacting partners that could bind to ARID3C. Further research is needed to investigate proteins that could potentially form complexes with ARID3C as a transcription factor. Additionally, our study has primarily focused on ARID3C expression in 293T cells and monocytes. Therefore, studies in the cells with higher baseline expression levels of ARID3C, such as in the liver or skin, will reveal further function in the future.

https://doi.org/10.1021/acs.jproteome.3c00509
J. Proteome Res. 2024, 23, 2882−2892

Previously, mass spectrometry (MS) could identify protein interactors but it was challenging to pinpoint the exact binding sites. In this study, we utilized deep learning to predict the interaction between ARID3C and NPM1, thereby revealing the precise binding sites, REKLES β domain with 4 specific 4 amino acids. Thus, by integrating deep learning with the experimental data, we were able to uncover a function of ARID3C. We also characterized the function of ARID3C in monocyte-to-macrophage differentiation and validated its role as a transcription factor using NPM1 as a nuclear shuttle. ARID3C bound to NPM1 leads to nucleus translocation and functions as a transcription factor regulating the expression of master transcription factors involved in monocyte to macrophage monocytic differentiation, including STAT3, STAT1, and JUNB.

■ ASSOCIATED CONTENT

Supporting Information

The Supporting Information is available free of charge at https://pubs.acs.org/doi/10.1021/acs.jproteome.3c00509.

Figure S1: Schematic representation of the plasmid construct. Figure S2: Identified MS spectra of ARID3C. Figure S3: STRING analysis of PPI networks for AIRD3C interactors. Figure S4: The 3D structure of ARID3C and NPM1 protein predicted by Alphafold2. Table S1: Information of used PCR primers and antibodies. (PDF)

■ AUTHOR INFORMATION

Corresponding Author

Je-Yoel Cho − *Department of Biochemistry, College of Veterinary Medicine, Research Institute for Veterinary Science, and BK21 FOUR Future Veterinary Medicine Leading Education and Research Center and Comparative Medicine Disease Research Center (CDRC), Science Research Center (SRC), Seoul National University, Seoul 08826, Republic of Korea;* orcid.org/0000-0003-1030-3577; Phone: +82-02-880-1268; Email: jeycho@snu.ac.kr; Fax: +82-02-886-1268

Authors

Hui-Su Kim − *Department of Biochemistry, College of Veterinary Medicine, Research Institute for Veterinary Science, and BK21 FOUR Future Veterinary Medicine Leading Education and Research Center and Comparative Medicine Disease Research Center (CDRC), Science Research Center (SRC), Seoul National University, Seoul 08826, Republic of Korea*

Yong-In Kim − *Department of Biochemistry, College of Veterinary Medicine, Research Institute for Veterinary Science, and BK21 FOUR Future Veterinary Medicine Leading Education and Research Center and Comparative Medicine Disease Research Center (CDRC), Science Research Center (SRC), Seoul National University, Seoul 08826, Republic of Korea;* Present Address: Cambridge Centre for Proteomics, Department of Biochemistry, University of Cambridge, Cambridge CB2 1QR, United Kingdom

Complete contact information is available at: https://pubs.acs.org/10.1021/acs.jproteome.3c00509

Author Contributions

H.-S.K. contributed to the design of the experiments, performed the experiments, analyzed the data, and wrote the first and revised draft of the paper. Y.-I.K. contributed revised the paper. J.-Y.C. conceived the idea, provided scientific direction, revised the paper extensively, and supervised the entire study.

Notes

The authors declare no competing financial interest.

■ ACKNOWLEDGMENTS

We thank the Korea Basic Science Institute (KBSI) for their mass spectrometric measurements. This research was supported by grants from the Ministry of Science and ICT and the National Research Foundation of Korea (NRF) SRC program: Comparative Medicine Disease Research Center (CDRC) (2021R1A5A1033157) and National Research Foundation of Korea (NRF) (2014M3A9D5A01073598).

■ ABBREVIATIONS

ARID3C, AT-rich interactive domain-containing protein 3C; NPM1, nucleophosmin 1; STAT3, signal transducer and activator of transcription 3; STAT1, signal transducer and activator of transcription 1; JUNB, JunB Proto-Oncogene; HLPC, high-performance liquid chromatography; MS, mass spectrometry; FDR, false discovery rate; hnRNPs, heterogeneous nuclear ribonucleoproteins; CD11b, cluster of differentiation molecule 11B; CSf1R, colony stimulating factor 1 receptor; CD14, cluster of differentiation molecule 14; PMA, phorbol 12-myristate 13-acetate; ChIP, chromatin immunoprecipitation; C-HPP, Chromosome-centric Human Proteome Project; uPE, uncharacterized PE1 protein; MP, missing protein; AML, acute myeloid leukemia; NES, nuclear export signal; NLS, nuclear localization signal; PU.1, Spi-1 Proto-Oncogene SPI1; CEBPA, CCAAT/enhancer-binding protein alpha; RUNX1, runt-related transcription factor 1; CTCF, CCCTC-binding factor; MIZ1, Myc-interacting zinc finger protein 1; HEXIM1, HEXIM P-TEFb complex subunit 1

■ REFERENCES

(1) Yates III, J. R. The revolution and evolution of shotgun proteomics for large-scale proteome analysis. *J. Am. Chem. Soc.* **2013**, *135* (5), 1629−1640.

(2) Doll, S.; Burlingame, A. L. Mass spectrometry-based detection and assignment of protein posttranslational modifications. *ACS Chem. Biol.* **2015**, *10* (1), 63−71.

(3) Karpievitch, Y. V.; Polpitiya, A. D.; Anderson, G. A.; Smith, R. D.; Dabney, A. R. Liquid chromatography mass spectrometry-based proteomics: biological and technological aspects. *Ann. Appl. Stat.* **2010**, *4* (4), 1797.

(4) Camperi, J.; Goyon, A.; Guillarme, D.; Zhang, K.; Stella, C. Multi-dimensional LC-MS: the next generation characterization of antibody-based therapeutics by unified online bottom-up, middle-up and intact approaches. *Analyst* **2021**, *146* (3), 747−769.

(5) Wen, B.; Zeng, W. F.; Liao, Y.; Shi, Z.; Savage, S. R.; Jiang, W.; Zhang, B. Deep learning in proteomics. *Proteomics* **2020**, *20* (21−22), 1900335.

(6) Bryant, P.; Pozzati, G.; Elofsson, A. Improved prediction of protein-protein interactions using AlphaFold2. *Nat. Commun.* **2022**, *13* (1), 1265.

(7) Jumper, J.; Evans, R.; Pritzel, A.; Green, T.; Figurnov, M.; Ronneberger, O.; Tunyasuvunakool, K.; Bates, R.; Žídek, A.; Potapenko, A.; et al. Highly accurate protein structure prediction with AlphaFold. *Nature* **2021**, *596* (7873), 583−589.

(8) Tidwell, J. A.; Schmidt, C.; Heaton, P.; Wilson, V.; Tucker, P. W. Characterization of a new ARID family transcription factor (Bright-like/ARID3C) that co-activates Bright/ARID3A-mediated immunoglobulin gene transcription. *Molecular immunology* **2011**, *49* (1−2), 260−272.
(9) Patsialou, A.; Wilsker, D.; Moran, E. DNA-binding properties of ARID family proteins. *Nucleic acids research* **2005**, *33* (1), 66−80.
(10) Kim, D.; Probst, L.; Das, C.; Tucker, P. W. REKLES is an ARID3-restricted multifunctional domain. *J. Biol. Chem.* **2007**, *282* (21), 15768−15777.
(11) Rhee, C.; Edwards, M.; Dang, C.; Harris, J.; Brown, M.; Kim, J.; Tucker, H. O. ARID3A is required for mammalian placenta development. *Developmental biology* **2017**, *422* (2), 83−91.
(12) Ward, J. M.; Ratliff, M. L.; Dozmorov, M. G.; Wiley, G.; Guthridge, J. M.; Gaffney, P. M.; James, J. A.; Webb, C. F. Human effector B lymphocytes express ARID3a and secrete interferon alpha. *Journal of autoimmunity* **2016**, *75*, 130−140.
(13) Shen, M.; Li, S.; Zhao, Y.; Liu, Y.; Liu, Z.; Huan, L.; Qiao, Y.; Wang, L.; Han, L.; Chen, Z.; et al. Hepatic ARID3A facilitates liver cancer malignancy by cooperating with CEP131 to regulate an embryonic stem cell-like gene signature. *Cell Death & Disease* **2022**, *13* (8), 732.
(14) Tang, J.; Yang, L.; Li, Y.; Ning, X.; Chaulagain, A.; Wang, T.; Wang, D. ARID3A promotes the development of colorectal cancer by upregulating AURKA. *Carcinogenesis* **2021**, *42* (4), 578−586.
(15) Dausinas, P.; Pulakanti, K.; Rao, S.; Cole, J. M.; Dahl, R.; Cowden Dahl, K. D. ARID3A and ARID3B induce stem promoting pathways in ovarian cancer cells. *Gene* **2020**, *738*, 144458.
(16) Hwang, H. J.; Lee, K. H.; Cho, J. Y. ABCA9, an ER cholesterol transporter, inhibits breast cancer cell proliferation via SREBP-2 signaling. *Cancer Science* **2023**, *114* (4), 1451.
(17) Park, H.-M.; Kim, H.; Kim, D. W.; Yoon, J.-H.; Kim, B.-G.; Cho, J.-Y. Common plasma protein marker LCAT in aggressive human breast cancer and canine mammary tumor. *BMB reports* **2020**, *53* (12), 664.
(18) Wiśniewski, J. R.; Zougman, A.; Nagaraj, N.; Mann, M. Universal sample preparation method for proteome analysis. *Nat. Methods* **2009**, *6* (5), 359−362.
(19) Lee, D.; Lee, K.-H.; Kim, D. W.; Yoon, S.; Cho, J.-Y. CXCL5 inhibits excessive oxidative stress by regulating white adipocyte differentiation. *Redox Biology* **2022**, *54*, 102359.
(20) Goddard, T. D.; Huang, C. C.; Meng, E. C.; Pettersen, E. F.; Couch, G. S.; Morris, J. H.; Ferrin, T. E. UCSF ChimeraX: Meeting modern challenges in visualization and analysis. *Protein Sci.* **2018**, *27* (1), 14−25.
(21) Maggi, L. B., Jr.; Kuchenruether, M.; Dadey, D. Y.; Schwope, R. M.; Grisendi, S.; Townsend, R. R.; Pandolfi, P. P.; Weber, J. D. Nucleophosmin serves as a rate-limiting nuclear export chaperone for the Mammalian ribosome. *Mol. Cell. Biol.* **2008**, *28* (23), 7050−7065.
(22) Huber, R.; Pietsch, D.; Günther, J.; Welz, B.; Vogt, N.; Brand, K. Regulation of monocyte differentiation by specific signaling modules and associated transcription factor networks. *Cellular and molecular life sciences* **2014**, *71*, 63−92.
(23) Ribechini, E.; Leenen, P. J.; Lutz, M. B. Gr-1 antibody induces STAT signaling, macrophage marker expression and abrogation of myeloid-derived suppressor cell activity in BM cells. *European journal of immunology* **2009**, *39* (12), 3538−3551.
(24) Coccia, E. M.; Russo, N. D.; Stellacci, E.; Testa, U.; Marziali, G.; Battistini, A. STAT1 activation during monocyte to macrophage maturation: role of adhesion molecules. *International immunology* **1999**, *11* (7), 1075−1083.
(25) Fontana, M. F.; Baccarella, A.; Pancholi, N.; Pufall, M. A.; Herbert, D. B. R.; Kim, C. C. JUNB is a key transcriptional modulator of macrophage activation. *J. Immunol.* **2015**, *194* (1), 177−186.
(26) Adhikari, S.; Nice, E. C.; Deutsch, E. W.; Lane, L.; Omenn, G. S.; Pennington, S. R.; Paik, Y.-K.; Overall, C. M.; Corrales, F. J.; Cristea, I. M. A high-stringency blueprint of the human proteome. *Nat. Commun.* **2020**, *11* (1), 5301.
(27) Baker, M. S.; Ahn, S. B.; Mohamedali, A.; Islam, M. T.; Cantor, D.; Verhaert, P. D.; Fanayan, S.; Sharma, S.; Nice, E. C.; Connor, M.; et al. Accelerating the search for the missing proteins in the human proteome. *Nat. Commun.* **2017**, *8* (1), 1−13.
(28) Falini, B.; Brunetti, L.; Sportoletti, P.; Martelli, M. P. NPM1-mutated acute myeloid leukemia: from bench to bedside. *Blood, The Journal of the American Society of Hematology* **2020**, *136* (15), 1707−1721.
(29) Falini, B.; Bolli, N.; Liso, A.; Martelli, M.; Mannucci, R.; Pileri, S.; Nicoletti, I. Altered nucleophosmin transport in acute myeloid leukaemia with mutated NPM1: molecular basis and clinical implications. *leukemia* **2009**, *23* (10), 1731−1743.
(30) Gu, X.; Ebrahem, Q.; Mahfouz, R. Z.; Hasipek, M.; Enane, F.; Radivoyevitch, T.; Rapin, N.; Przychodzen, B.; Hu, Z.; Balusu, R. Leukemogenic nucleophosmin mutation disrupts the transcription factor hub that regulates granulomonocytic fates. *J. Clin. Invest.* **2018**, *128* (10), 4260−4279.
(31) Wang, A. J.; Han, Y.; Jia, N.; Chen, P.; Minden, M. D. NPM1c impedes CTCF functions through cytoplasmic mislocalization in acute myeloid leukemia. *Leukemia* **2020**, *34* (5), 1278−1290.

https://doi.org/10.1021/acs.jproteome.3c00509
J. Proteome Res. 2024, 23, 2882−2892